Isolation of Polycavernoside D from Marine Cyanobacterium

Gabriel Navarro †, Susie Cummings †, John Lee †, Nathan Moss †, Evgenia Glukhov †, Frederick A. Valeriote, ‡ Lena Gerwick †, William H. Gerwick *†§

† Center for Marine Biotechnology and Biomedicine, Scripps Institution of Oceanography and Skaggs School of Pharmacy and Pharmaceutical Sciences, University of California at San Diego, La Jolla, California 92093, United States
‡ Henry Ford Health System, Department of Internal Medicine, Josephine Ford Cancer Center, Detroit, Michigan 48202, United States
§ Skaggs School of Pharmacy and Pharmaceutical Sciences, University of California, San Diego, La Jolla, California 92093, United States

Contents

• Supporting Methods

• Supplemental Data

• References.

Abbreviation List:

(CD)	Circular dichroism
(NMR)	Nuclear magnetic resonance
(DQF-COSY)	Double-quantum filtered correlation spectroscopy
(TOCSY)	Total correlation spectroscopy
(ROESY)	Rotating-frame Overhauser effect spectroscopy
(HSQC)	Heteronuclear single quantum coherence
(HMBC)	Heteronuclear multiple bond correlation
(MS)	Mass spectrometry
(LTQ-FT-ICR)	Linear ion trap Fourier transform ion cyclotron resonance
(MS/MS)	Tandem mass spectrometry
(VLC)	Vacuum-liquid chromatography
(HPLC)	High performance liquid chromatography
(SPE)	Solid phase extraction
(DCM)	Dichloromethane
(MeOH)	Methanol
(ACN)	Acetonitrile
(DMSO)	Dimethyl sulfoxide
($CDCl_3$)	Deuterated chloroform
(CD_3CN)	Deuterated acetonitrile
(MTT)	3-(4,5-dimethylthiazol-2-yl)-2,5-diphenyltetrazolium bromide

General experimental procedures. Optical rotations were measured on a JASCO P-2000 polarimeter, circular dichroism (CD) measurements were obtained on an AVIV-125, and UV spectra were obtained on a Beckman Coulter DU-800 spectrophotometer. Nuclear magnetic resonance (NMR) spectra were recorded with solvent peaks as internal standards (δC 77.0, δH 7.26 for $CDCl_3$ and δC 118.3, δH 1.94 for CD3CN) on a Bruker Avance III 600 MHz spectrometer with a 1.7 mm inverse detection triple resonance (H-C/N/D) cryoprobe (600 and 151 MHz for ^{1}H and ^{13}C NMR, respectively). For 1D NMR experiements, number of scans was set to 8. For 2D NMR experiments, the number of scans (nt) was set to 32 while the number of free induction decay increments (ni) was set to 256. Pulse sequences used were standard preloaded Bruker pulse sequences. Mass spectrometery data was collected using a Triversa nanomate-electrospray ionization source (Advion Biosystems) coupled to a 6.42 T Thermo linear ion trap Fourier transform ion cyclotron resonance (LTQ-FT-ICR) mass spectrometer (MS). Syringe flow rate was set to 1 μL/min with samples at 0.1 μM concentrations. Tandem mass spectrometry (MS/MS) data were averaged over 22 scans. All solvents were either distilled or of high performance liquid chromatography (HPLC) quality.

Extraction, isolation and chemical characterization. Macroscopic filaments of a red-colored benthic cyanobacterium were collected by hand in shallow water (1 m) near Punto de Vistas, Puerto Rico in 2011. Biomass was stored at -20°C for three months before solvent extraction. The crude lipophilic extract (#2126) was generated by extracting the dried biomass 3x with 200 mL of dichloromethane:methanol (2:1) via sconication for 30 minutes. The recombined organic extracts were dried under vacuum, then fractionated using vacuum-liquid chromatography (VLC) (SI Figure 2) to yield 9 fractions. These fractions were subsequently screened against a suite of mammalian cancer cell lines.[1] The second most polar VLC fraction (2126-H) showed potent and selective activity against murine solid tumor cell line colon38, but was only modestly cytotoxic against murine leukemia cell line L1210 as well as normal untransformed cells (SI Table 1). Fraction 2126-H was further fractionated into five fractions with a Gracepure™ solid phase extraction (SPE) C18-max 5000 mg column using a 20% methanol stepped gradient, and submitted to a cytotoxicity assay using the H-460 human lung cancer cell line (SI Figure 3).[2] Fraction 2126-H-5 (100% methanol) showed the highest cytotoxicity at both 30 and 3 μg/mL, and was thus selected for HPLC purification of major constituent, polycavernoside D (0.3 mg, 8.5% of 2126-H-5). RP HPLC [5 μ Kinetex C18, 65% acetonitrile (ACN)−H_2O over 50 min] purification of 100% MeOH SPE fraction (2126-H-5) produced pure polycavernoside D (**1**, 0.3 mg).
Polycavernoside D (**1**): White powder; $[\alpha]^{23}_{D}$ -1 (c 0.63, ACN); CD (0.15 mM, ACN) λmax (Δε) 260.0 nm (-1.07), 271.0 (-1.14), 282.0 (-0.98); UV (CH3CN) λmax 260 (5.69), 270 (5.80), 280 (5.70) nm; ^{1}H and ^{13}C NMR see SI Table 2. HRESIMS $[M+Na]^+$ m/z 833.4313 (calcd for $C_{42}H_{66}NaO_{15}$ 833.4299).

16s rRNA taxanomic identification: Genomic DNA was isolated using a QIAGEN genomic DNA isolation kit. DNA concentration and purity were determined using a DU-800 spectrophotometer (Beckman Coulter). The 16S rRNA gene was PCR-amplified from the isolated genomic DNA using the 16S specific primers, 27F1(UFP) 5'-TAGTGTAAAACGACGGCCAGTAGAGTTTGATCCTGGCTCAG-3' and 1509R 5'-GGCTACCTTGTTACGACTT-3'.[3, 4] The PCR reaction volumes were 25.5 μL containing 2.5 μL (~ 200 ng) of DNA, 12.5 μL of 2x Taq Polymerase Master Mix, 9.5 μL of sterilized water, and 1.0 μL of each forward and reverse primer from a stock of 10 μM concentration. The PCR reactions were performed in an Eppendorf Mastercycler gradient as follows: initial denaturation for 2 min at 95 °C, 30 cycles of amplification (30 s at 95 °C, 20 s at 48 °C, and 130 s at 72 °C), and final elongation for 3 min at 72 °C. PCR products were immediately ligated into Life Technologies pCR™-4-TOPO® TA vectors per manufacturer's directions via the TOPO® TA Cloning® Kit for sequencing. Vectors were transformed into TOP10 competent cells and grown overnight on selective agarose media. Single colonies were picked for PCR reaction to confirm correct ligation, using M13 primers, and overnight culturing in 5 mL LB with 100 μg/mL ampicillin. Plasmid DNA was isolated from transformants using the QIAprep Spin Miniprep kit (Qiagen) and Sanger sequenced with M13 forward and reverse primers. VQR-28MAR11-2 accession: KT013096. Closest match accession: GU724195.1

Supplemental Data

Figure S1. Microscopic images of the collected environmental sample of *Okeania* sp. VQR28MAR11-2. The sample was preserved in RNAlater solution, and images taken on an Olympus IX51 epifluorescent microscope (100×, 20x, 4x) with an Olympus U-CMAD3 camera.

4x Magnification

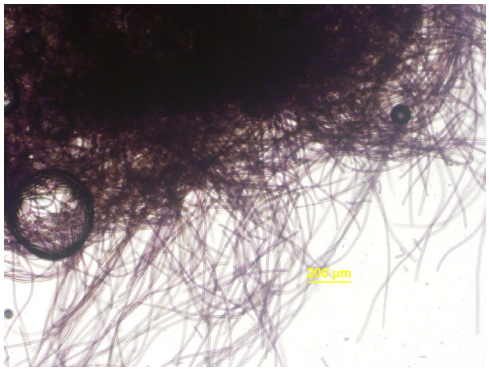

20x Magnification

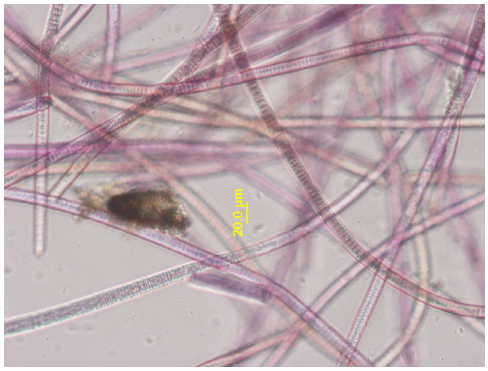

100x Magnification

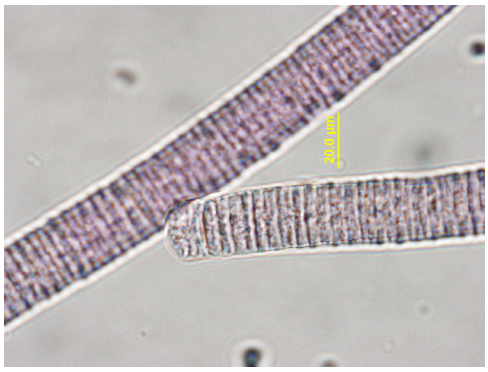

Figure S2. VQR28MAR11-2 vacuum liquid chromatography (VLC) and C18-SPE fractionation scheme for the isolation of polycavernoside D.

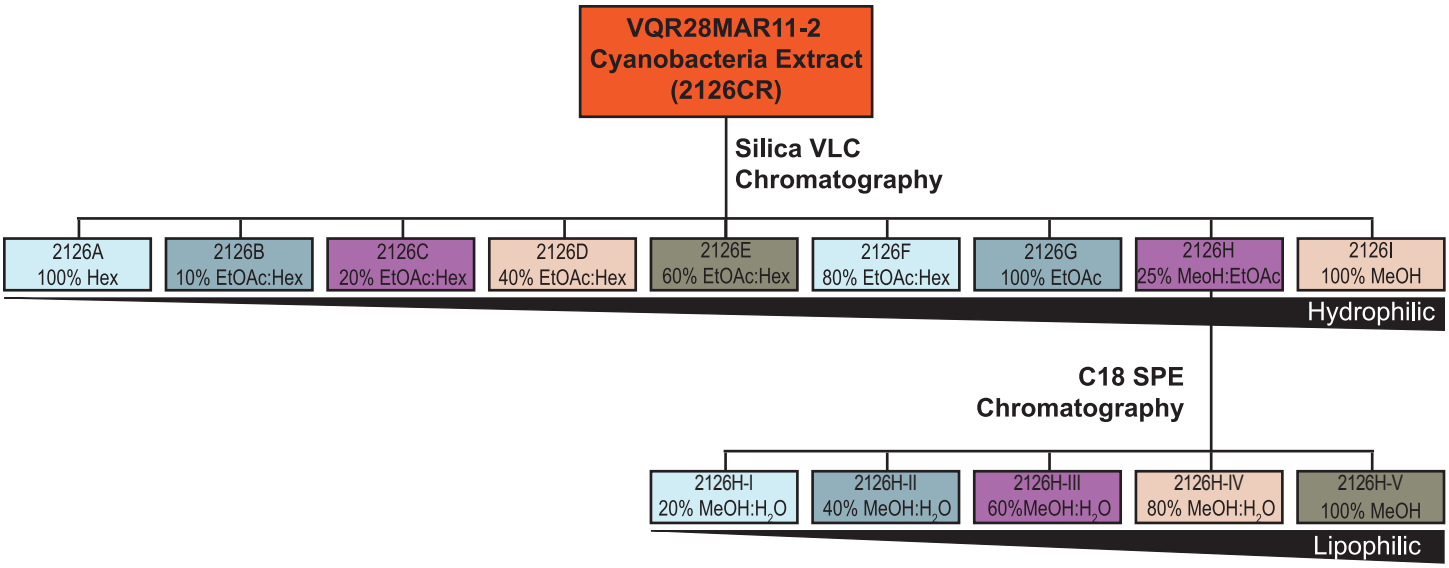

Figure S3. H-460 cytotoxicity assay results for 2126H SPE fractions. Roman numerals correspond to the SPE fraction shown in Figure S2. SPE fractions were screened with doxorubicin as a positive control.

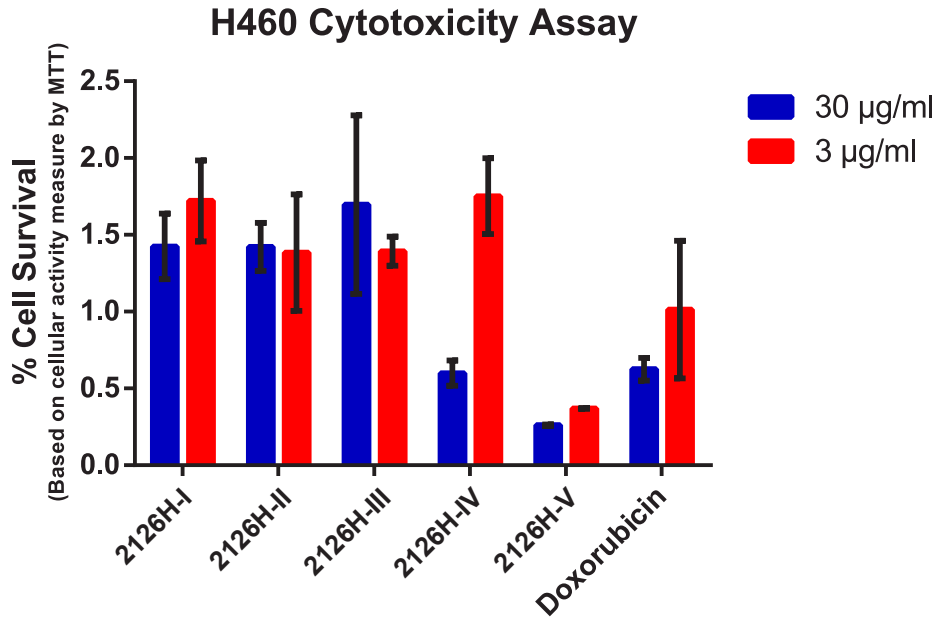

Figure S4. Tandem mass spectrometry (MS/MS) analysis of polycavernoside D. Shown in red are the resulting fragmentations of polycavernoside D corresponding to the fragmentations depicted in the structure to the left.

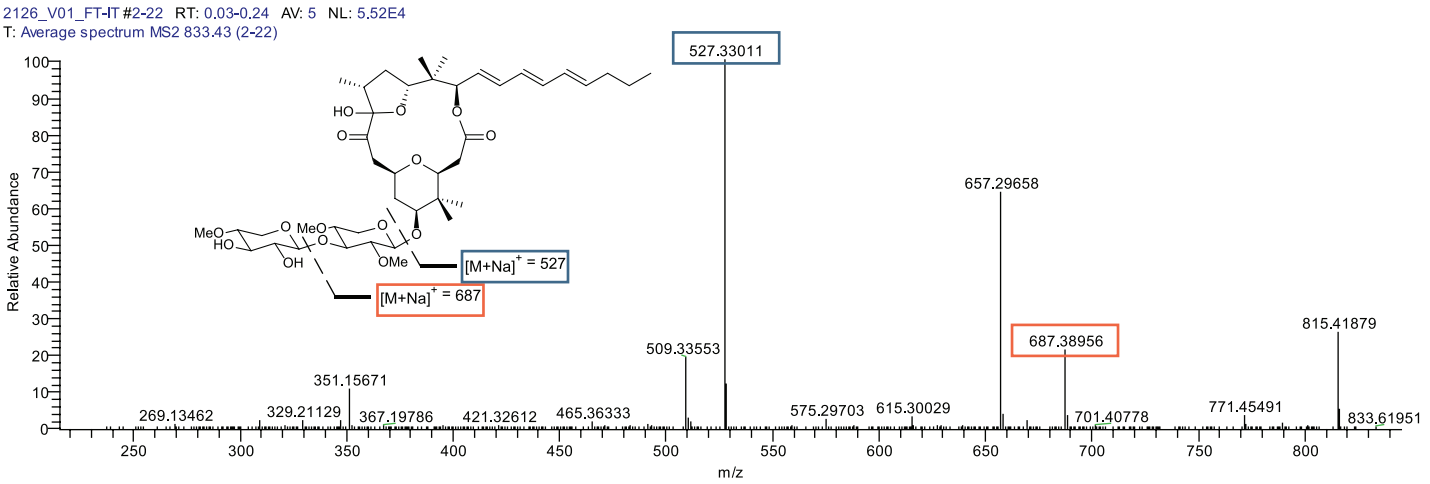

Figure S5. Circular dichroism (CD) spectrum comparison of polycavernoside A and D. Polycavernoside A CD spectrum was adapted from [5].

Polycavernoside D: CD (CH_3CN, 0.15 mM) λ_{ext} 260.0 nm ($\Delta\varepsilon$ -1.07), 271.0 (-1.14), 282.0 (-0.98)

Natural Polycavernoside A: CD (CH_3CN, 0.66 mM) λ_{ext} 210 nm ($\Delta\varepsilon$ 0.71), 227.8 (- 0.15), 246.0 (0.21), 258.6 (0.03), 260.8 (0.15), 269.6 (- 0.63), 280.4 (- 0.65) 299.0 (-0.78)

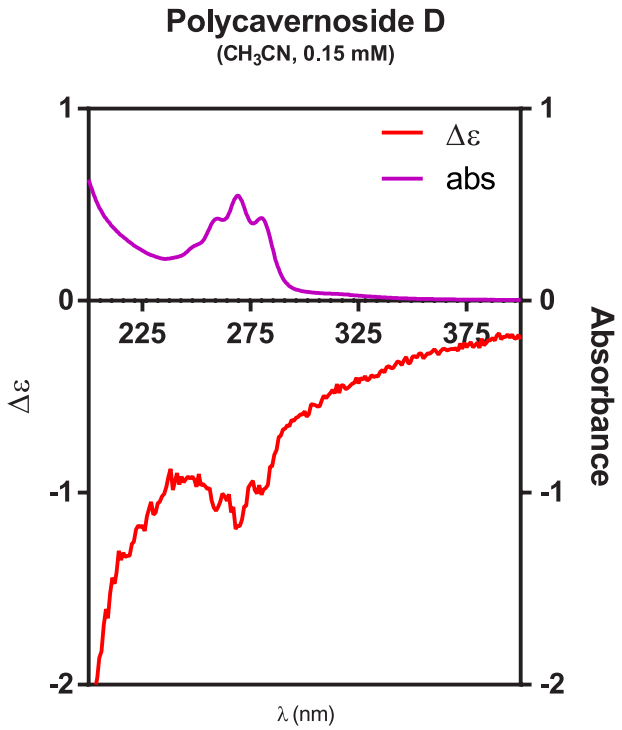

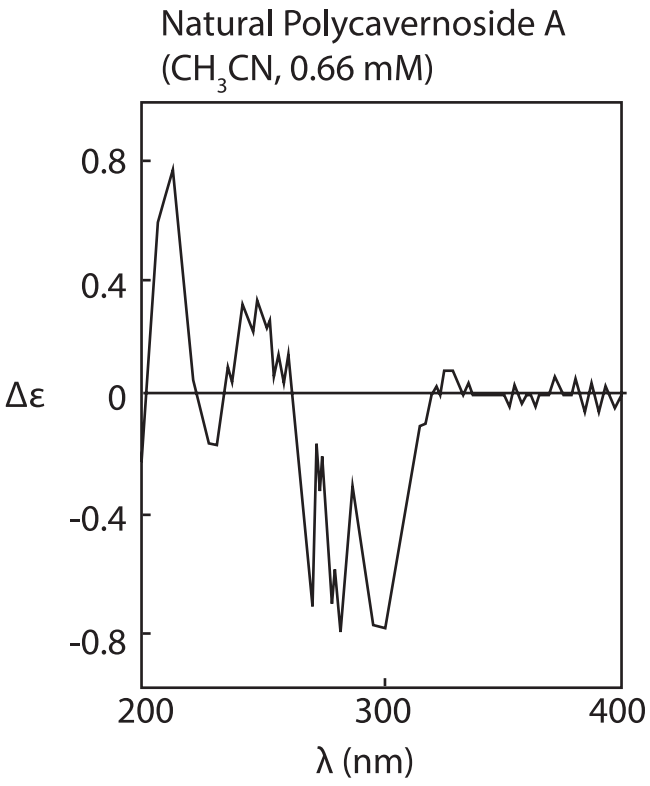

Figure S6. Dose response curve for polycavernoside D against H-460 cells. Screened with doxorubicin as a positive control.

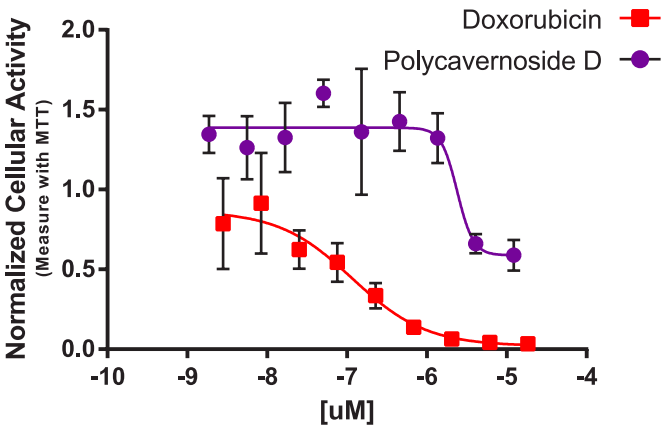

Figure S7. NMR data set for polycavernoside D in deuterated chloroform.

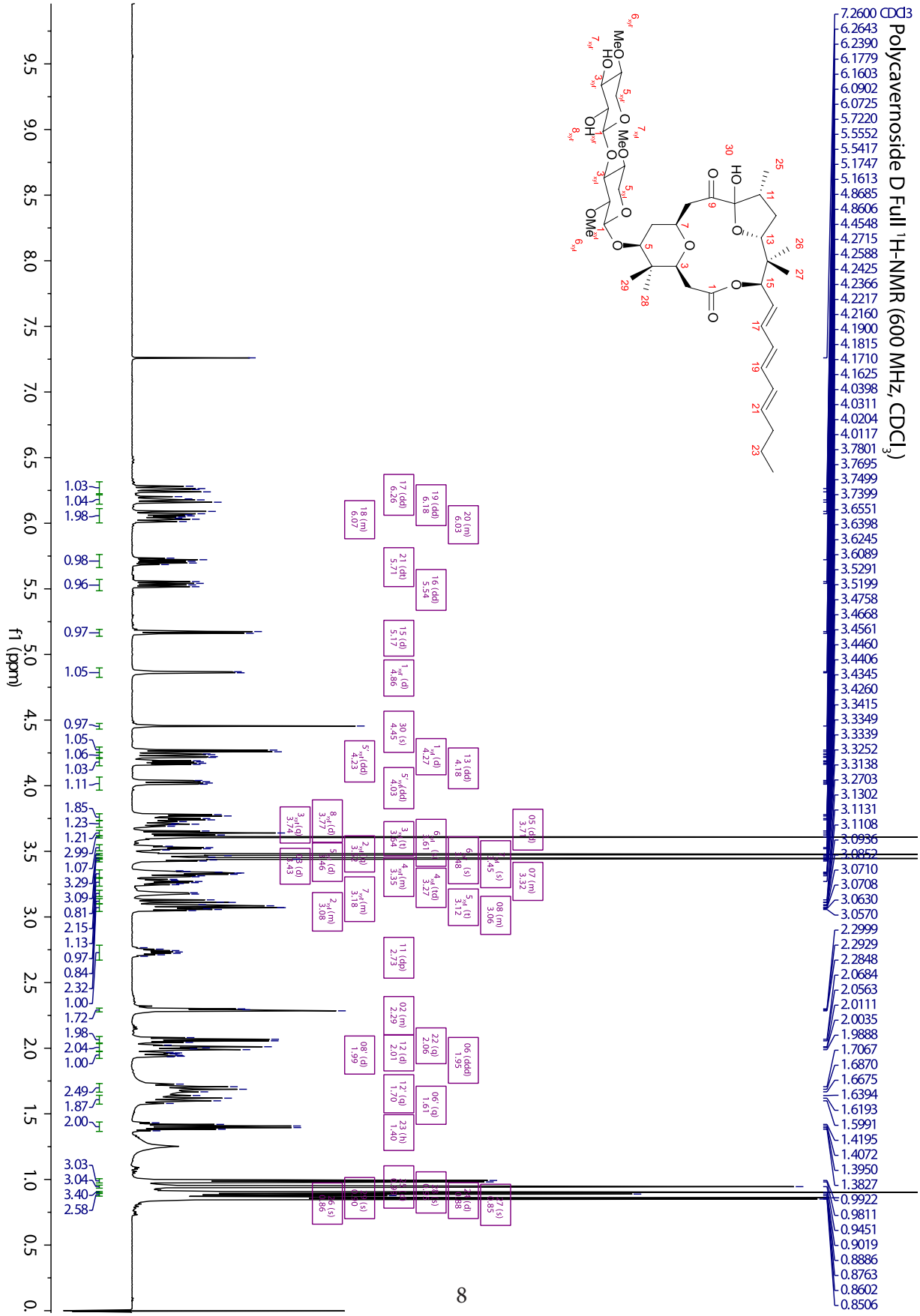

Polycavernoside D Zoom ^{1}H-NMR (600 MHz, $CDCl_3$)

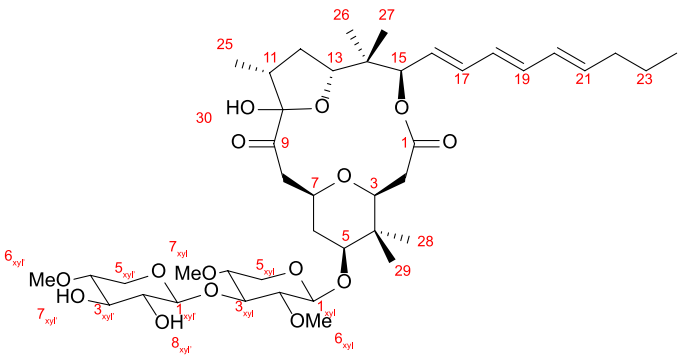

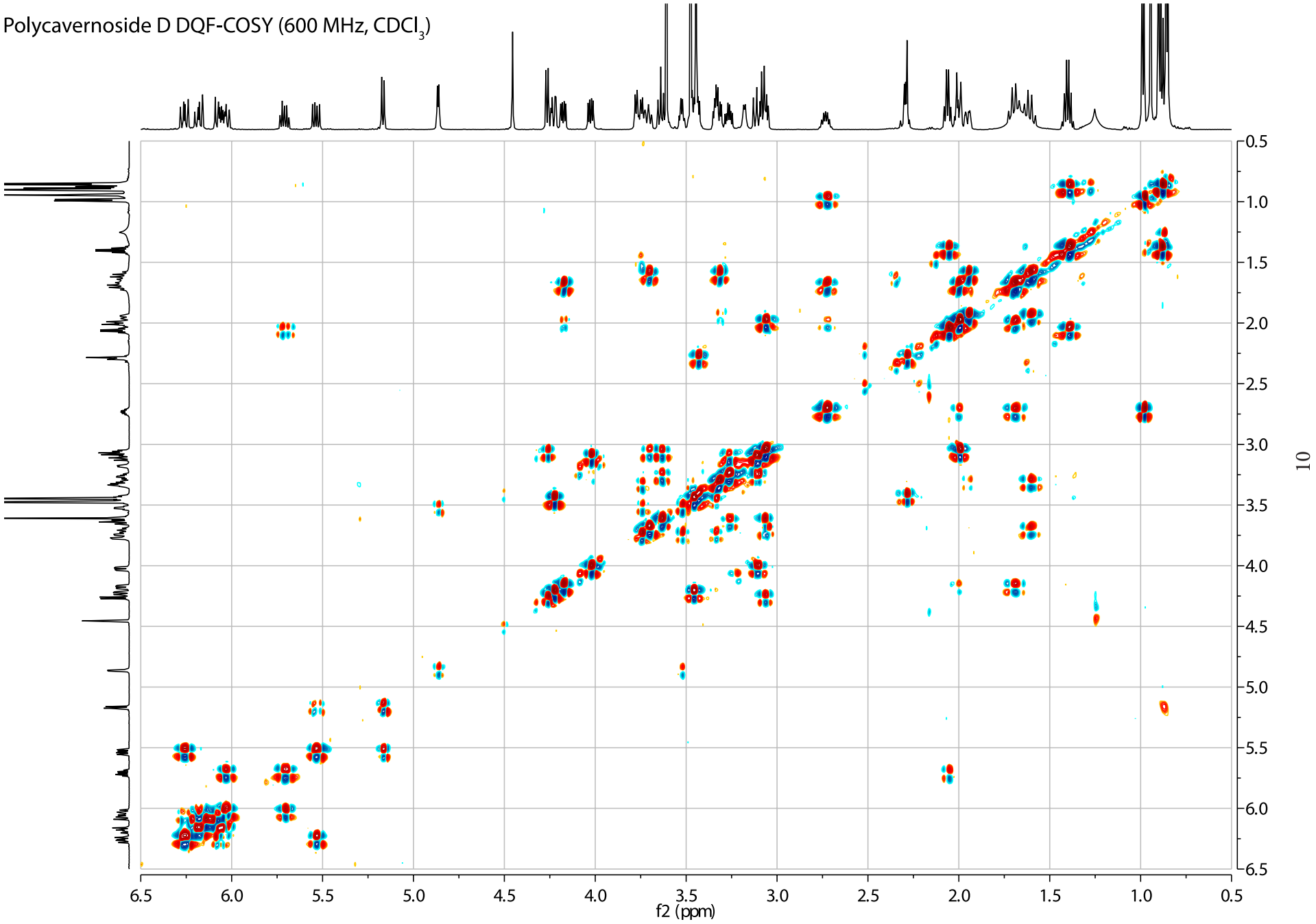
Polycavernoside D DQF-COSY (600 MHz, CDCl3)
6.5
6.0
5.5
5.0
4.5
4.0
3.5
3.0
2.5
2.0
1.5
1.0
0.5
f2 (ppm)
10

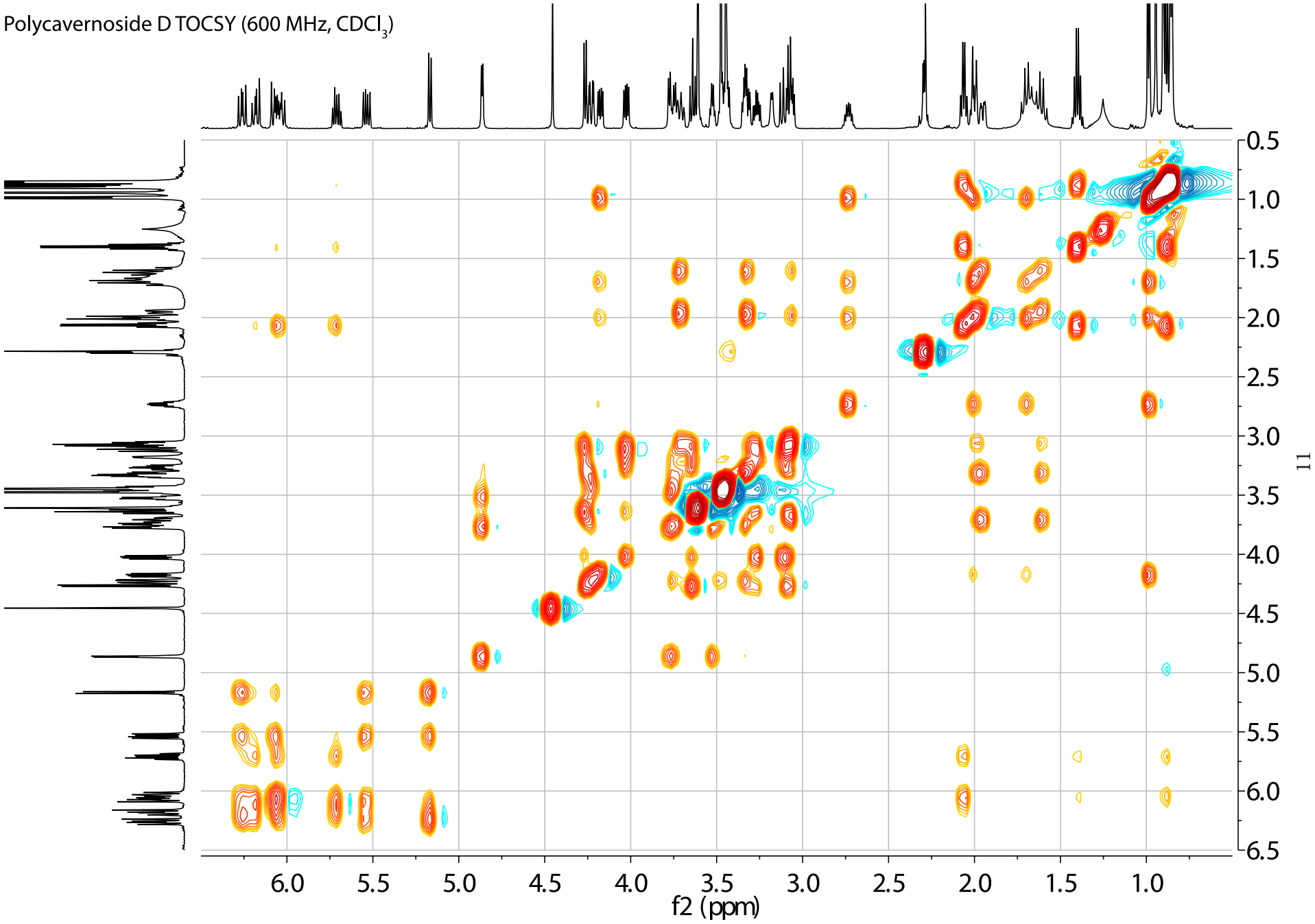
Polycavernoside D TOCSY (600 MHz, CDCl3)
6.0
5.5
5.0
4.5
4.0
3.5
3.0
2.5
2.0
1.5
1.0
f2 (ppm)
0.5
1.0
1.5
2.0
2.5
3.0
3.5
4.0
4.5
5.0
5.5
6.0
6.5
11

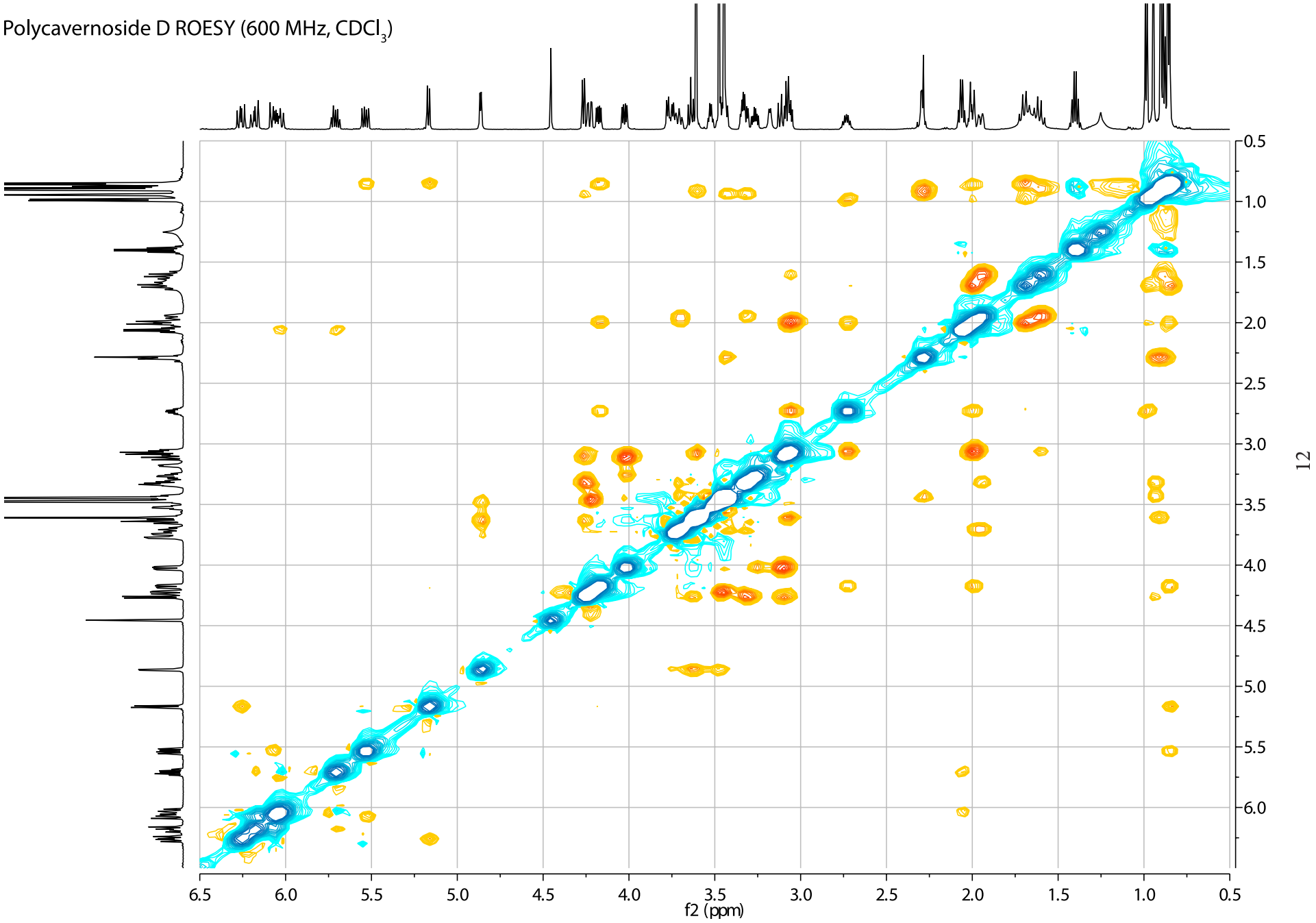
Polycavernoside D ROESY (600 MHz, CDCl3)
6.5
6.0
5.5
5.0
4.5
4.0
3.5
3.0
2.5
2.0
1.5
1.0
0.5
f2 (ppm)
0.5
1.0
1.5
2.0
2.5
3.0
3.5
4.0
4.5
5.0
5.5
6.0
12

Polycavernoside D HSQC (600 MHz, $CDCl_3$)

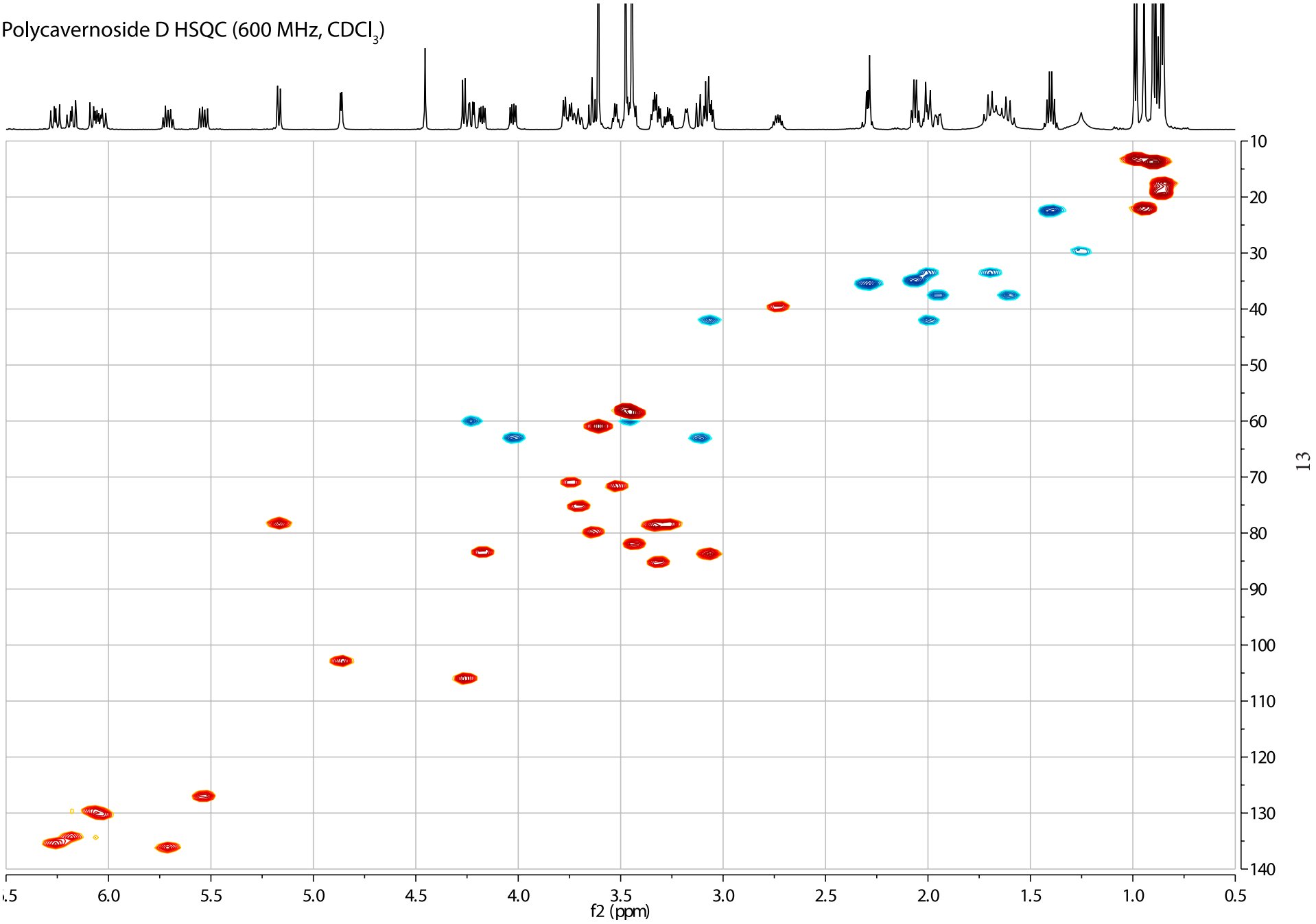

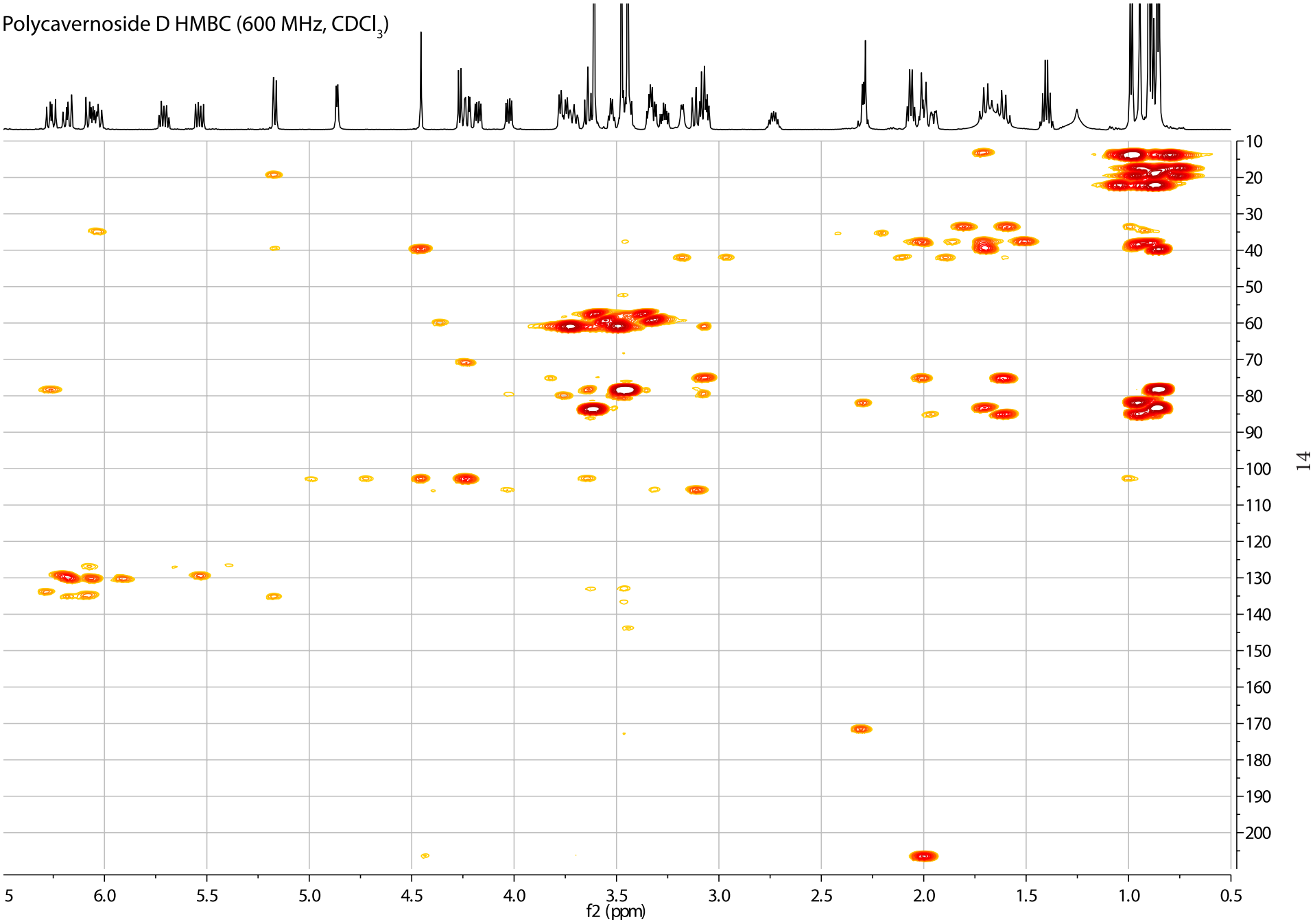
Polycavernoside D HMBC (600 MHz, CDCl3)
f2 (ppm)
14

Table S1. Vacuum liquid chromatography (VLC) disk diffusion assay results from crude extract 2126. In red are fractions with notable selective inhibitory activity to murine colon38 cell line. The radius of oabserved cell growth inhibition was measured in millimeters. Cell lines: mouse lymphocytic leukemia L1210; mouse colon carcinoma Colon38; murine colony forming unit granulocyte monocyte CFU-GM; human colon carcinoma HCT116; human lung carcinoma H125; human breast adenocarcinoma MCF-7; human prostatic carcinoma LNCaP; human ovarian adenocarcinoma OVC-5; glioblastoma U251N; human breast adenocarcinoma MDA; human lymphoblastic leukemia CEM.

		Murine			Human								
Number	Dilution	L1210	Colon38	CFU-GM	HCT116	H125	MCF-7	LNCaP	OVC-5	U251N	PANC-1	MDA	CEM
2126 A	1		100		0	0	0	0	0	0	0	0	
2126 B	1		150		0	50	50	0	0	0	0	0	
2126 C	1		200		100	100	50	50	100	0	100	50	
2126 D	1		200		100	50	100	100	150	50	150	100	
2126 E	1	200	300	150	150	100	100	100	200	100	200	100	
2126 F	1	300	150	250	200	150	200	300	200	100	200	150	200
2126 G	1	**350**	**650**	**300**	200	200	300	300	250	250	400	300	350
	1	**350**	**700**	**250**									
2126 H	1	**400**	**>1000**	**700**	400	250	350	400	500	450	**650**	550	**350**
	1										**600**		**300**
	1/4	**300**	**>1000**	**450**									
	1/16	**100**	**>1000**	**600**									
2126 I	1	200	0	150	100	0	0	0	150	50	100	0	
2126 CR	1		0		0	50	150	100	100	50	100	100	

Table S2. ^{1}H and ^{13}C NMR comparison of polycavernoside A and D in deuterated chloroform and acetonitrile. NMR value for polycavernoside A dapted from [6]

	Polycavernoside D in $CDCl_3$			Polycavernoside D in CD_3CN			Polycavernoside A in CD_3CN		
Position	δ_C	Type	δ_H (*J* in Hz)	δ_C	Type	δ_H (*J* in Hz)	δ_C	Type	δ_H (*J* in Hz)
1	171.5	C	-	172.5	C	-	172.1	C	-
2	35.5	CH_2	2.29 m	36.1	CH_2	2.28 dd (12.8, 11.1)	40.2	CH_2	2.14 dd (12, 12)
2'	35.5	CH_2	2.29 m	36.1	CH_2	2.33 dd (12.7, 3.2)	40.2	CH_2	2.52 dd (12, 3)
3	81.9	CH	3.43 dd (5.08)	82.6	CH	3.37 dd (11.5, 2.8)	79.8	CH	3.29 td (12, 3)
4	38.2	C	-	40.1	C	-	42.7	CH	1.27 m
5	75.1	CH	3.71 dd (12.0, 9.2)	85.3	CH	3.41 dd (10.8, 4.8)	82.7	CH	3.33 td (11, 4)
6	37.5	CH_2	1.61 ddd (12.0, 12.0, 12.0)	37.8	CH_2	1.63 ddd (16.8, 16.8, 4.8)	41.5	CH_2	1.37 q (11)
6'	37.5	CH_2	1.97 ddd (12.8, 4.7, 2.4)	37.8	CH_2	1.86 ddd (12.9, 4.8, 2.5)	41.5	CH_2	2.05 dd (11, 4)
7	85.1	CH	3.32 m	76.1	CH	3.61 dddd (13.2, 10.8, 7.8, 3.0)	79.3	CH	3.64 (brt 11)
8	42.0	CH_2	1.99 m	42.4	CH_2	2.10 dd (13.8, 4.1)	43	CH_2	2.07 d (14)
8'	42.0	CH_2	3.06 m	42.4	CH_2	3.04 dd (13.8, 8.5)	43	CH_2	2.97 dd (14, 9)
9	206.5	C	-	207.7	C	-	207.4	C	-
10	102.6	C	-	103.9	C	-	103.9	C	-
11	39.5	CH	2.73 ddq (6.8, 6.7, 6.7)	39.6	CH	2.79 ddq (9.5, 9.5, 7.1)	39.5	CH	2.76 m
12	33.5	CH_2	1.70 ddd (11.7, 11.7, 11.7)	34.1	CH_2	1.59 ddd (16.2, 16.2, 4.8)	34.2	CH_2	1.56 q (12)
12'	33.5	CH_2	2.01 m	34.1	CH_2	2.00 ddd (11.7, 6.7, 5.0)	34.2	CH_2	1.98 m
13	83.3	CH	4.18 dd (11.4, 5.1)	83.7	CH	4.11 dd (11.4, 5.0)	83.7	CH	4.05 dd (15, 5)
14	39.7	CH	-	40.4	CH	-	40.5	CH	-
15	78.3	CH	5.17 d (8.09)	78.9	CH	5.02 d (7.7)	78.9	CH	5.00 d (7)
16	126.9	CH	5.54 dd (15.1, 8.1)	128.8	CH	5.63 dd (15.9, 7.7)	128.7	CH	5.58 dd (15, 7)
17	135.5	CH	6.26 dd (15.2, 10.6)	135.5	CH	6.21 dd (15.8, 11.0)	135.3	CH	6.15 dd (15, 10)
18	129.6	CH	6.07 m	130.6	CH	6.14 m	130.6	CH	6.10 dd (15, 10)
19	134.2	CH	6.18 dd (14.9, 10.6)	134.8	CH	6.22 dd (16.2, 9.8)	128.1	CH	6.17 dd (15,10)
20	130.2	CH	6.03 m	131.3	CH	6.09 dd (15.8, 10.4)	134.8	CH	6.02 ddd (15, 10, 1)
21	136.2	CH	5.71 dt (14.7, 7.1)	136.9	CH	5.76 dt (14.8, 7.1)	143.7	CH	5.70 dd (15, 6)
22	35.0	CH_2	2.06 q (7.2)	35.4	CH_2	2.06 td (12.0, 3.6)	31.9	CH	2.99 sep d (6, 1)
23	22.4	CH_2	1.40 h (7.3)	23.0	CH_2	1.40 tq (7.3, 7.2)	-	-	-
24	13.2	CH_3	0.89 t (7.4)	13.8	CH_3	0.89 t (7.4)	22.4	CH_3	0.95 d (6)
25	13.7	CH_3	0.99 d (6.7)	13.4	CH_3	0.93 d (6.7)	13.6	CH_3	0.90 d (7)
26	17.6	CH_3	0.86 s	17.7	CH_3	0.82 s	18.2	CH_3	0.79 s
27	19.2	CH_3	0.85 s	19.3	CH_3	0.83 s	19.4	CH_3	0.78 s
28	22.0	CH_3	0.95 s	22.1	CH_3	0.93 s	12.8	CH_3	0.93 d (7)
29	13.7	CH_3	0.90 s	13.8	CH_3	0.87 s	-	-	-
30	-	OH	4.45 s	-	OH	4.59 s	-	OH	-
31	-	-	-	-	-	-	22.4	CH_3	0.95 d (6)
	Xylose			Xylose			Xylose		
1	106.0	CH	4.27 d (7.6)	106.4	CH	4.30 d (7.7)	106.2	CH	4.32 d (8)
2	83.7	CH	3.08 dd (7.6, 9.2)	84.9	CH	2.99 dd (9.1, 7.6)	85.4	CH	2.88 dd (10, 8)
3	79.9	CH	3.64 dd (9.2, 9.2)	81.3	CH	3.58 dd (8.9, 8.9)	79.8	CH	3.44 dd (10, 10)
4	78.4	CH	3.27 ddd (9.6, 9.5, 5.2)	79.0	CH	3.22 ddd (10.0, 8.9, 5.3)	78.9	CH	3.13 ddd (10, 10, 4)
5	63.1	CH_2	3.12 dd (11.6, 9.6)	63.7	CH_2	3.11 dd (11.5, 10.0)	63.6	CH_2	3.07 dd (10, 10)
5'	63.1	CH_2	4.03 dd (11.6, 5.2)	63.7	CH_2	3.93 dd (11.4, 5.3)	63.6	CH_2	3.93 dd (10, 4)
6	60.9	CH_3	3.61 s	61.0	CH_3	3.55 s	60.8	CH_3	3.48 s
7	58.6	CH_3	3.45 s	59.0	CH_3	3.39 s	58.5	CH_3	3.31 s
	Xylose			Xylose			Arabanose		
1	102.9	CH	4.86 d (4.8)	104.2	CH	4.63 d (6.6)	97.8	CH	5.21 d (4)
2	71.6	CH	3.52 ddd (5.9, 5.9, 5.9)	80.1	CH	3.17 m	78.2	CH	3.36 dd (11, 4)
3	71.0	CH	3.74 ddd (6.0, 6.0, 6.0)	74.9	CH	3.42 ddd (9.0, 7.2, 7.2)	79.9	CH	3.37 d (11)
4	78.7	CH	3.35 m	74.3	CH	3.18 m	69.5	CH	3.79 br s
5	60.0	CH_2	3.46 m	62.0	CH_2	3.17 m	66.1	CH	4.13 q (7)
5'	60.0	CH_2	4.23 dd (12.4, 3.5)	62.0	CH_2	4.04 dd (17.4, 10.8)	-	-	-
6	58.0	CH_3	3.48 s	58.5	CH_3	3.41 s	57	CH_3	3.34 s
7	-	OH	3.77 d (6.4)	-	OH	3.53 s	-	OH	-
8	-	OH	3.18 d (6.0)	-	OH	3.40 s	-	-	-
9	-	-	-	-	-	-	16.4	CH_3	1.07 d (7)
10	-	-	-	-	-	-	58.8	CH_3	3.38 s

References

[1] Valeriote, F.; Grieshaber, C. K.; Media, J.; Pietraszkewicz, H.; Hoffmann, J.; Pan, M.; McLaughlin, S. Discovery and development of anticancer agents from plants. *Journal of Experimental Therapeutics and Oncology*. **2002**, *2*, 228–236. doi: 10.1046/j.1359-4117.2002.01038.x

[2] Villa, F. A.; Lieske, K.; Gerwick, L. Selective MyD88-dependent pathway inhibition by the cyanobacterial natural product malyngamide F acetate. *European Journal of Pharmacology*. **2010**, *629*, 140–146.

[3] Neilan, B. A.; Jacobs, D.; Del Dot, T.; Blackall, L. L.; Hawkins, P. R.; Cox, P. T.; Goodman, A. E. rRNA sequences and evolutionary relationships among toxic and nontoxic cyanobacteria of the genus Microcystis. *International Journal of Systematic Bacteriology*. **1997**, *47*, 693–697. doi: 10.1099/00207713-47-3-693

[4] Martinez-Murcia, A. J.; Acinas, S. G.; Rodriguez-Valera, F. Evaluation of prokaryotic diversity by restrictase digestion of 16S rDNA directly amplified from hypersaline environments. *FEMS Microbiology Ecology*. **1995**, 17, 247–255. doi: 10.1016/0168-6496(95)00029-A

[5] Fujiwara, K., Murai, A., Yotsu-Yamashita, M., & Yasumoto, T. Total Synthesis and Absolute Configuration of Polycavernoside A. *Journal of the American Chemical Society*. **1998**, *120*, 10770–10771. doi:10.1021/ja982431b

[**6**] Yotsu-Yamashita, M., Haddock, R. L., & Yasumoto, T. (1993). Polycavernoside A: a novel glycosidic macrolide from the red alga Polycavernosa tsudai (Gracilaria edulis). *Journal of the American Chemical Society*. **1993**, *115*, 1147–1148. doi:10.1021/ja00056a048